Research Paper

# Brd4 inhibition attenuates unilateral ureteral obstruction-induced fibrosis by blocking TGF-β-mediated Nox4 expression

Baoshang Zhou[a,1], Jiao Mu[a,1], Yi Gong[b], Caibao Lu[a], Youguang Zhao[c], Ting He[a], Zhexue Qin[d,*]

[a] Department of Nephrology, Xinqiao Hospital, Third Military Medical University, Chongqing 400037, China
[b] Department of Nephrology, Southwest Hospital, Third Military Medical University, Chongqing 400038, China
[c] Department of Urology, Chengdu Military General Hospital, Chengdu 610083, China
[d] Department of Cardiology, Xinqiao Hospital, Third Military Medical University, Chongqing 400037, China

## ARTICLE INFO

## ABSTRACT

Uncovering new therapeutic targets for renal fibrosis holds promise for the treatment of chronic kidney diseases. Bromodomain and extra-terminal (BET) protein inhibitors have been shown to effectively ameliorate pathological fibrotic responses. However, the pharmacological effects and underlying mechanisms of these inhibitors in renal fibrosis remain elusive. In this study, we determined that the inhibition of Brd4, a BET family member, with a selective potent chemical inhibitor, JQ1, could prevent the development of renal fibrosis and block the progression of fibrosis in rats that have undergone unilateral ureteral obstruction (UUO). Inhibiting Brd4 with either JQ1 or genetic knockdown resulted in decreased expression of fibrotic genes such as α-smooth muscle actin, collagen IV and fibronectin both in UUO-induced fibrosis and upon TGF-β1 stimulation in HK-2 cells. Brd4 inhibition also suppressed the oxidative stress induced by UUO in vivo or by TGF-β1 in HK-2 cells. Moreover, Nox4, which is constitutively active in renal cells and is involved in the generation of hydrogen peroxide, was up-regulated during UUO-mediated fibrosis and induced by TGF-β1 in HK-2 cells, and this up-regulation could be blunted by Brd4 inhibition. Consistently, Nox4-mediated ROS generation and fibrotic gene expression were attenuated upon Brd4 inhibition. Further, the transcriptional activity of Nox4 was suppressed by JQ1 or siRNA against Brd4. Additionally, Smad3 and ERK1/2 phosphorylation, which are upstream signals of Nox4 expression, were inhibited both in JQ1-administered UUO rats and Brd4-inhibited HK-2 cells. In conclusion, these results indicated that the inhibition of Brd4 might protect against renal fibrosis by blocking the TGF-β-Nox4-ROS-fibrosis axis, suggesting that Brd4 could be a promising therapeutic target.

## 1. Introduction

Renal fibrosis is a common pathway that is activated as a result of different renal injuries and subsequent chronic kidney diseases (CKD). Renal interstitial fibrosis is characterized by tubulointerstitial fibroblast proliferation and extracellular matrix (ECM) deposition in the kidney parenchyma. Evidence suggests that transforming growth factor-β (TGF-β) is an important mediator in the development and progression of interstitial fibrosis [1,2]. Increased TGF-β1 leads to Smad2/3 phosphorylation and nuclear translocation and ultimately the activation of target fibrotic gene expression [3]. Given the potent role of TGF-β signaling, the elucidation of novel mechanisms during renal fibrosis holds the promise of finding new therapeutic targets for this disease.

The bromodomain and extra-terminal (BET) family consists of the Brd2, Brd3, Brd4, and testis-specific Brdt proteins that have two conserved N-terminal bromodomains (BD1 and BD2). BET proteins recognize acetylated histones and act as readers of protein acetylation by binding to acetylated lysine residues through BD1 and BD2 to govern transcriptional activity. Meanwhile, the extra-terminal and C-terminal domains of BET proteins can bind to transcription factors and chromatin histone modifiers, thus recruiting these co-regulators to promoter or enhancer sites to modulate gene transcription [4].

A well-studied member of the BET family, Brd4 recruits positive transcription elongation factor b (p-TEFb) to the transcription start site and modulates RNA polymerase II (RNA pol II) activity [5,6]. In addition, Brd4 has been implicated in NF-κB-mediated inflammation through its interaction with the NF-κB subunit RelA in renal cell lines and upon experimental renal damage [7–10]. Additionally, Brd4 has been found to associate with the oncogene c-MYC through their co-

occupancy of promoter and enhancer elements to regulate cell proliferation [11]. Small-molecule BET inhibitors such as JQ1 and I-BET mimic the acetyl moiety, compete with the acetyllysine-binding pocket and disassociate BET proteins from chromatin [12]. JQ1 and other BET inhibitors disproportionately suppress specific genes and exert potent effects on cancer proliferation, cell cycle progression and inflammation. Several studies have shown that JQ1 might also participate in tissue fibrosis. JQ1 mitigated bleomycin-induced murine lung fibrosis [13] and pressure overload-induced cardiac fibrosis [14]. Suarez-Alvarez et al. reported that JQ1 alleviated unilateral ureteral obstruction (UUO)-induced kidney inflammation [10]; however, whether JQ1 could reduce tubulointerstitial fibrosis remains unknown.

Reactive oxygen species (ROS) play an important role in the pathogenesis of renal fibrosis and can be initiated by TGF-β/Smad signaling. NADPH oxidases are the major source of ROS in renal cells in both physiological and pathological conditions. Among the Nox isoforms, Nox4 has been characterized as constitutively active in cells, and its expression determines the levels of ROS, particularly hydrogen peroxide [15]. Previous studies have shown that Nox4 is highly expressed in the kidney and contributes to renal pathology [15,16]. Nox4 plays an important role in TGF-β-induced ROS generation and mediates myofibroblast differentiation to the pro-fibrotic phenotype, which is essential to renal fibrosis [16,17]. The regulation of Nox4 by TGF-β1 has also been well established in various cell types [18], including tubular cells, which contribute to the development and progression of renal fibrosis. However, whether Brd4 is involved in the TGF-β-induced ROS generation in renal fibrosis is still unknown.

Here, we aimed to investigate whether Brd4 inhibition could modulate UUO-induced experimental fibrosis in the kidney. Meanwhile, we sought to determine the potential mechanisms involved in the effects of Brd4 inhibition on TGF-β signaling and Nox4-mediated ROS generation.

## 2. Methods

### 2.1. Reagents and antibodies

JQ1 was purchased from Tocris Bioscience (Bristol, UK). The recombinant human TGF-β1 was from PeproTech (Rocky Hill, NJ, USA). Antibodies used in Western blot and sources were as follows. The rabbit anti-Brd4 antibody was supplied by Santa Cruz Biotechnology (Santa Cruz, CA, USA). Rabbit anti-α-SMA, anti-fibronectin and anti-collagen IV antibodies were purchased from Abcam (Cambridge, UK). Rabbit anti-Smad3, anti-p-Smad3, anti-ERK1/2, anti-p-ERK1/2 and anti-Nox4 antibodies were purchased from Cell Signaling Technology (Danvers, MA, USA). The rabbit anti-GAPDH antibody was from Bioss (Beijing, China). DCFH-DA was from Beyotime Biotechnology (Jiangsu, China), Amplex Red Hydrogen Peroxide/Peroxidase Assay Kit from Molecular Probes (Eugene, OR, USA), polyethylene glycol (PEG)–catalase and N-acetyl-cysteine (NAC) from Sigma-Aldrich (St. Louis, MO, USA), SIS3 from Cayman Chemical (Ann Arbor, MI, USA), and U0126 from Santa Cruz Biotechnology (Santa Cruz, CA, USA).

### 2.2. Experimental animals and UUO model

Adult male Sprague Dawley rats weighing 150–180 g were housed under controlled temperature conditions in a 12 h light–dark cycle in the Center for Experimental Animals in Xinqiao Hospital. The animals were allowed free access to water and standard chow. UUO was performed as we have previously described [19]. Briefly, the rats were anesthetized with an intramuscular injection of 100 mg/kg ketamine and 5 mg/kg xylazine. The left ureter was exposed, and the lower and upper ends were then ligated with 3-0 silk sutures. In the sham group, the ureter was stripped but not ligated or cut. The UUO rats were divided into groups injected intraperitoneally with 100 mg/kg JQ1

daily (n=6 each). The vehicle control rats were given an equal amount of DMSO in carrier solution. The rats were euthanized on day 1, day 7 or day 14 after the UUO surgery. The left kidneys were collected, rinsed with ice-cold normal saline, dissected and fixed in 10% neutral buffered formalin or stored in liquid nitrogen for further analysis. All experimental procedures were in compliance with the National Institutes of Health Guide for the Care and Use of Laboratory Animals and approved by the Institutional Animal Care and Use Committee of Third Military Medical University.

### 2.3. Cell culture

The immortalized human proximal tubular epithelial cell line HK-2 was procured from the American Type Culture Collection (ATCC, Manassas, VA, USA). The cells were cultured in low glucose (1 g/L) Dulbecco's Modified Eagle's Medium/F12 (DMEM/F12) containing 10% FBS and antibiotics at 37 °C in 5% $CO_2$. The cells used in the experiments were grown to approximately 80% confluence. Prior to stimulation, HK-2 cells were maintained in serum-free medium for 24 h.

### 2.4. Quantitative real-time PCR

Total RNA was isolated from HK-2 cells or frozen kidney tissues using RNAiso Plus (TaKaRa Biotech, Dalian, China) per the manufacturer's instructions and subjected to reverse transcription into cDNA with a PrimeScript™ RT Reagent Kit (TaKaRa Biotech, Dalian, China ). The quantitative real-time PCR analysis was performed using an ABI ViiA7DX System (Foster City, CA, USA). GAPDH expression was used as the internal reference in all PCR experiments. The RT-PCR primers designed for specific target genes are listed in Supplemental Table I and were synthesized by TaKaRa Biotech. The PCR reactions were performed using following cycling conditions: 95 °C for 30 s, followed by 40 cycles of 95 °C for 5 s, 60 °C for 30 s and 72 °C for 20 s.

### 2.5. Western blot analysis

HK-2 cells and renal tissues were lysed with RIPA buffer containing protease inhibitors (Beyotime, Jiangsu, China) to obtain the total proteins. The protein samples were separated on SDS polyacrylamide gels and transferred to PVDF membranes, and the membranes were then blocked with 5% fat-free milk and immunoblotted with primary antibodies. The primary antibodies were used at the following dilutions: anti-Brd4 (1:500), anti-Nox4 (1:500), anti-α-SMA (1:2000), anti-fibronectin (1:1000), anti-collagen IV (1:500), anti-Smad3 (1:1000), anti-phospho-Smad3 (1:500), anti-ERK (1:1000), anti-phospho-ERK1/2 (1:1000) and anti-GAPDH (1:1000). After incubation with an appropriate secondary antibody, the western blots were visualized using the Chemiluminescent HRP Substrate (Millipore, Billerica, MA, USA). The data analysis was performed using ImageJ Software (NIH, USA) to quantify the levels of proteins.

### 2.6. Histology staining and immunohistochemistry

Sections (4 µm thick) from 10% formalin-fixed, paraffin-embedded kidney tissues were used for hematoxylin and eosin staining and Masson's trichrome staining. The ratio of the fibrotic area was assessed by outlining the blue staining of five randomly selected microscopic fields from each kidney using Image-Proplus software. Immunohistochemistry was performed using a Polink-1 one-step polymer detection system (ZSGB-BIO, Beijing, China). Briefly, the kidney sections were stained with anti-α-SMA (Beyotime, Jiangsu, China), anti-Brd4 (Abcam, Cambridge, UK), anti-fibronectin (Abcam, Cambridge, UK), and anti-collagen IV (Abcam, Cambridge, UK) antibodies, followed by incubation with secondary antibodies, and then detected with the EnVision/HRP Kit (Dako, Denmark).
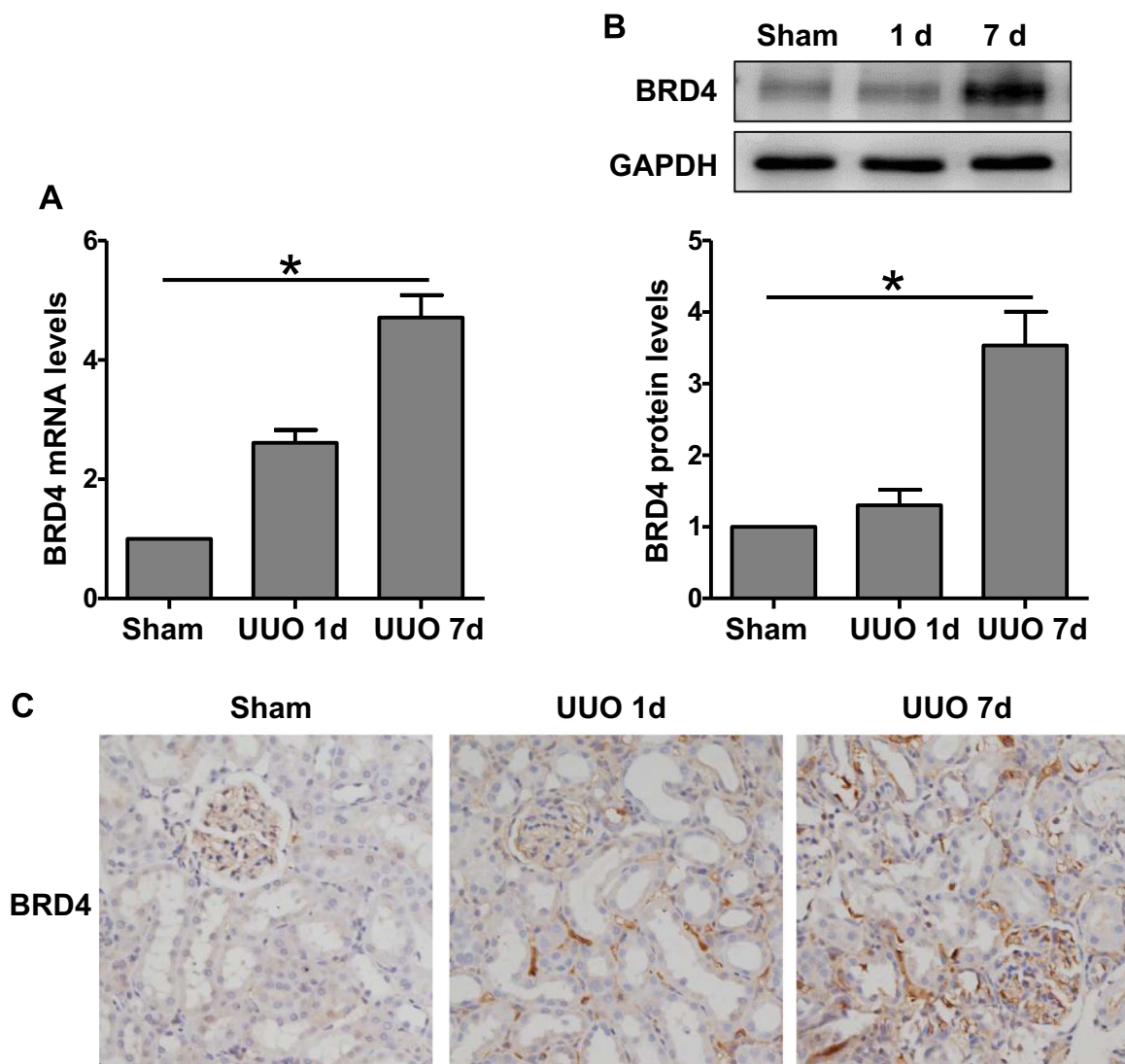
**Fig. 1.** Brd4 was up-regulated in the kidney after unilateral ureteral obstruction (UUO). (A) Brd4 mRNA levels were detected by real-time RT-PCR at day 1 and 7 after UUO. (B) Brd4 protein levels were detected by western blot analysis at day 1 and 7 after UUO. (C) Immunohistochemical staining of Brd4 in renal sections at day 1 and 7 after UUO. Values are expressed as the mean ± SEM. *$P < 0.05$, relative to the sham group, n=3.

### 2.7. Small interfering RNA (siRNA) transfection

HK-2 cells were transfected with siRNAs specific to Brd4 or Nox4 or with non-targeting siRNAs (Santa Cruz, CA, USA) as a negative control for 48 h using Lipofectamine 3000 reagent (Invitrogen, Carlsbad, CA, USA). All siRNAs were used at a concentration of 100 nM. After 6 h of transfection, the cells were incubated in DMEM/F12 containing 0.2% FBS for 48 h. Real-time PCR was conducted to confirm the effects of siRNA transfection.

### 2.8. Adenoviral infection

HK-2 cells at 70–80% confluence were infected with adenovirus to overexpress human Nox4 (a gift from Dr. Tong, Chongqing University, China) at an MOI of 50 in DMEM without serum or antibiotics for 6 h before switching to DMEM/F12 containing 10% FBS for 72 h.

### 2.9. Luciferase reporter assays

The Nox4 promoter reporter vector was designed and synthesized by Sangon Biotech (Shanghai, China). The reporter construct was transiently transfected along with a Renilla control plasmid and either

Brd4 siRNA or non-targeting siRNAs using Lipofectamine 3000 reagent (Invitrogen) according to the manufacturer's instructions. At 6 h after transfection, the culture medium was replaced with DMEM/F12 supplemented with 0.2% FBS. After 48 h of transfection, the HK-2 cells were then treated with 10 ng/mL TGF-β1. The luciferase activity was detected using a dual-luciferase reporter assay system (Promega, Madison, WI, USA). Three independent experiments were performed, with six replicates for each condition.

### 2.10. Measurement of ROS production

Intracellular ROS levels were determined by incubation with dichlorodihydrofluorescein diacetate (DCFH-DA). HK-2 cells were treated with 20 μM DCFH-DA in Hanks' balanced salt buffer for 30 min at 37 °C. The dichlorofluorescein fluorescence was visualized by confocal fluorescence microscopy and measured at excitation and emission wavelengths of 530 nm and 580 nm, respectively.

### 2.11. Amplex Red assay for $H_2O_2$ production

For the detection of $H_2O_2$, an Amplex Red assay was performed as we have previously described [20]. Briefly, $H_2O_2$ production was

measured by Amplex Red in HK-2 cells cultured in DMEM//F12 containing 0.2% FBS. The HK-2 cells were treated with or without 10 ng/mL TGF-β1 for 24 h. For specific cases, HK-2 cells were pre-treated with JQ1, Brd4 siRNA or Nox4 siRNA and then treated with or without 10 ng/mL TGF-β1 for 24 h. To detect the kidney tissue $H_2O_2$ levels, the kidneys were first perfused and homogenized as previously described [15]. The hydrogen peroxide in the homogenate was measured using Amplex Red (100 μM) with 10 U/mL horseradish peroxidase, according to the manufacturer's suggestions (Molecular Probes). Fluorescent readings were obtained from the rat kidneys after 1 h of incubation at 37 ºC, and the values were normalized to the protein amount as measured by a Bradford assay. The Amplex Red reagent is a colorless substrate that reacts with $H_2O_2$ with a 1:1 stoichiometry to produce the highly fluorescent resorufin (excitation/emission maxima=570/585 nm).

### 2.12. Statistical analysis

All values are expressed as the mean ± SEM unless otherwise stated. The statistical analysis of the difference between two groups was performed using Student's t-test. Comparisons among groups were analyzed using a one-way ANOVA followed by a Student-Newman-Keuls test. A P-value < 0.05 was considered statistically significant.

## 3. Results

### 3.1. Up-regulation of Brd4 in the progression of renal fibrosis after UUO

We first examined the expression of Brd4 in renal interstitial fibrosis. Both the mRNA and protein levels of Brd4 were enhanced significantly in the UUO kidneys compared with the sham-operated kidneys (Fig. 1A and B). The elevation of Brd4 was observed at day 1 and increased by 3.53 ± 0.47-fold at day 7. To clarify the localization of the Brd4 protein, an immunohistochemical analysis was carried out with an anti-Brd4 antibody. Brd4 staining was observed in the tubular interstitium, and the density increased with the progression of renal fibrosis over time (Fig. 1C). These results indicated that Brd4 might participate the development of kidney fibrosis after UUO.

### 3.2. Brd4 inhibitor JQ1 attenuated renal fibrosis after UUO

JQ1, a well-recognized Brd4 inhibitor, was used to investigate whether Brd4 inhibition prevents renal fibrosis. In rats that underwent UUO, the interstitial fibrosis in renal tissue was remarkable, as observed by staining with HE and Masson' Trichrome (Fig. 2A). Treating rats with JQ1 for 7 days right after the UUO operation resulted in a less significant interstitial inflammation response and a lower fibrosis score (Fig. 2B and C). In addition, JQ1 inhibited interstitial α-SMA, collagen IV and fibronectin expression at both the mRNA and protein levels (Fig. 2D−G).

We next tested the effects of JQ1 during fibrosis progression. UUO rats treated with JQ1 from day 7 after the operation again showed decreased interstitial fibrosis at day 14 (Fig. 3A−D, Supplementary Fig. S1). Similarly, JQ1 reduced the α-SMA, collagen IV and fibronectin expression at day 14 in the JQ1 group compared with the vector group (Fig. 3E−G). Taken together, these results suggested that JQ1 treatment not only prevented renal fibrosis but also delayed the progression of established fibrosis.

### 3.3. TGF-β1-induced renal fibrosis depends on oxidative stress in vitro

ROS has been considered to be a mediator in the development of renal fibrosis [21,22]. Here, we measured the ROS generated upon TGF-β1 stimulation. The total ROS detected with the fluorescent dye

DCFH-DA showed that treatment with 10 ng/mL TGF-β1 caused ROS accumulation in the HK-2 cells (Fig. 4A). Hydrogen peroxide, one type of ROS, was markedly increased in a concentration-dependent manner (Fig. 4B). Concomitantly, the expression of fibrotic markers, such as α-SMA, collagen IV and fibronectin, was up-regulated significantly by TGF-β1 in a concentration-dependent manner (Fig. 4C and D). Further, the ablation of ROS with either NAC or PEG-catalase inhibited the TGF-β1-induced profibrogenic protein expression (Fig. 4E and F). Therefore, TGF-β1 induced renal fibrosis through oxidative stress.

### 3.4. Brd4 was involved in TGF-β1-induced fibrosis and oxidative stress in vitro

In HK-2 cells, JQ1 markedly inhibited TGF-β1-induced fibrotic gene expression, and this inhibitory effect occurred in a dose-dependent manner (Fig. 5A−C). To inhibit Brd4 genetically, siRNA was used. As shown in Supplementary Fig. S2, we observed a highly efficient knockdown of Brd4 gene expression after transfecting cells with an siRNA against Brd4. Similarly, the expression of profibrogenic proteins was markedly suppressed in the Brd4 knockdown group compared with the negative control siRNA group (Fig. 5D−F). These results implied that Brd4 participates in TGF-β1-induced fibrosis gene expression.

As mentioned above, TGF-β1-induced ROS production activates fibrosis. Therefore, we further investigated whether Brd4 inhibition could suppress TGF-β1-induced ROS generation. JQ1 significantly decreased the TGF-β1-mediated induction of hydrogen peroxide (Fig. 5G) and total ROS (Fig. 5H). Brd4 knockdown also resulted in reduced ROS generation compared with the control group (Fig. 5G and H). These results indicated that the protective effects of Brd4 inhibition could be attributed to reduced fibrosis and oxidative stress.

### 3.5. Brd4 inhibition blocked TGF-β1-induced oxidative stress and fibrosis through Nox4

Nox4, a member of Nox family, has been reported to be the major Nox isoform involved in hydrogen peroxide and total ROS production. Consistent with previous reports [23], TGF-β1 induced Nox4 expression in HK-2 cells (Fig. 6A), while not affecting Nox1 or Nox2 levels (Supplementary Fig. S3). In HK-2 cells, we detected lower levels of the fibrotic proteins after Nox4 knockdown (Fig. 6A). Nox4 knockdown also significantly reduced hydrogen peroxide generation in TGF-β1-treated HK-2 cells (Fig. 6B). These data demonstrated the critical role of Nox4 in TGF-β1-induced oxidative stress and fibrosis.

We next examined the effects of Brd4 inhibition on Nox4 expression. As shown in Fig. 6C and D, JQ1 blocked TGF-β1-induced Nox4 expression at both the mRNA and protein levels. Likewise, Brd4 knockdown resulted in Nox4 down-regulation compared with the negative control group (Fig. 6C and D). To further investigate whether Brd4 regulates oxidative stress and fibrosis through Nox4, we compensated the JQ1-mediated Nox4 reduction by delivering an adenovirus carrying human Nox4 to HK-2 cells (Supplementary Fig. S4). The compensation of Nox4 blunted the JQ1-induced reduction of fibrotic protein levels and hydrogen peroxide production in HK-2 cells pretreated with TGF-β1 (Fig. 6E and F). Therefore, these results demonstrated that Brd4 inhibition exerts an anti-oxidative stress and anti-fibrotic role through the regulation of Nox4.

### 3.6. Brd4 regulated Nox4 expression via the Smad and ERK pathways

To further explore the underlying mechanisms responsible for the regulation of Nox4 by Brd4, we examined the possible pathways involved. Smad and ERK1/2 have been reported to play a pivotal role in Nox4-mediated renal fibrosis. Brd4 inhibition attenuated TGF-β1-induced Smad3 phosphorylation (Fig. 7A). ERK1/2 phosphorylation was also blocked by JQ1 when HK-2 cells were treated with TGF-β1
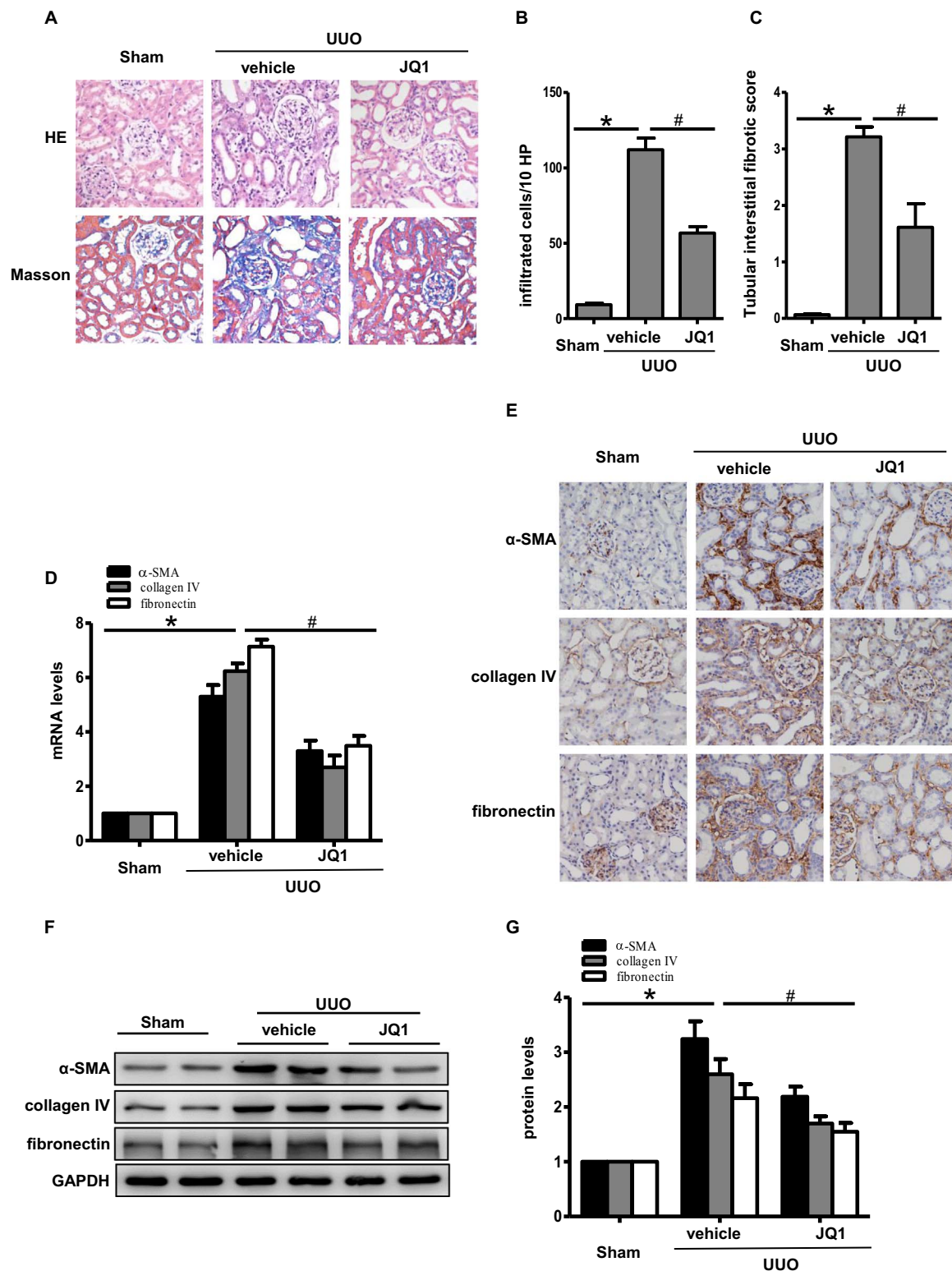
**Fig. 2.** JQ1 attenuated renal fibrosis after UUO. (A) Representative images of hematoxylin and eosin (HE) and Masson's trichrome staining at day 7 in UUO kidneys treated as indicated (n=6). (B) Bar graph quantification of infiltrated cells in the renal interstitium. (C) Bar graph quantification of renal tubular interstitial fibrotic scores. (B & C) Randomly selected image fields from six independent kidney samples were used for quantification. (D) Real-time PCR analyses for the mRNA expression of collagen IV, α-SMA and fibronectin in the UUO kidneys (n=3). (E) Representative images of immunohistochemical staining of collagen IV, α-SMA, fibronectin in the indicated groups (n=6). (F) Western blots of collagen IV, α-SMA, fibronectin at day 7 after UUO. (G) Bar graph showing the fold changes of collagen IV, α-SMA, fibronectin relative to sham group from three independent samples. Values are expressed as the mean ± SEM. *$P < 0.05$, relative to sham group; #$P < 0.05$, relative to vehicle control.

(Fig. 7B). Consistently, Brd4 knockdown led to the blockade of Smad and ERK1/2 signaling (Fig. 7A and B). Meanwhile, chemical inhibitors against Smad3 or ERK1/2 resulted in reduced Nox4 expression upon TGF-β1 stimulation (Fig. 7C).

Previously, TGF-β1 was reported to regulate Nox4 expression transcriptionally and significantly increase Nox4 promoter activity.
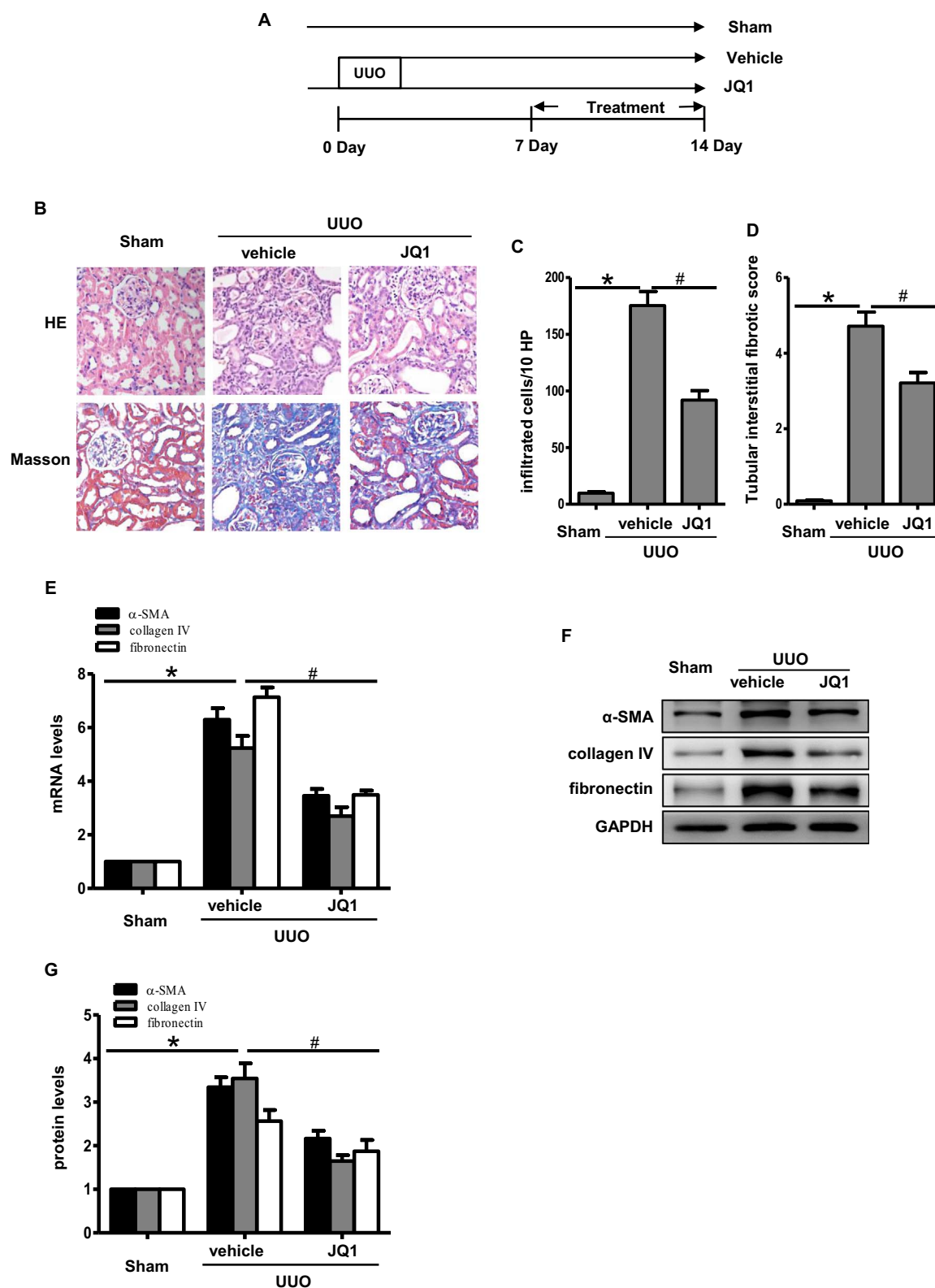
**Fig. 3.** JQ1 delayed the progression of renal fibrosis. (A) Experimental scheme for investigating the effects of JQ1 during renal fibrosis progression. (B) Representative images of HE and Masson's trichrome staining at day 14 in UUO kidneys treated as indicated. (C) Bar graph quantification of infiltrated cells in the renal interstitium. (D) Bar graph quantification of renal tubular interstitial fibrotic scores. (E) Real-time PCR analyses for the mRNA expression of collagen IV, α-SMA, fibronectin at day 14 in the UUO kidneys. Bar graphs represent three independent samples, each performed in triplicates. (F & G) On day 14 after UUO, collagen IV, α-SMA and fibronectin were detected by Western blot and quantitative analysis of results from three independent samples. Values are expressed as the mean ± SEM. *$P < 0.05$, relative to sham group; #$P < 0.05$, relative to vehicle control.

To further confirm that Brd4 could regulate TGF-β1-induced Nox4 expression, we transfected HK-2 cells with a luciferase reporter plasmid containing the human Nox4 promoter region. A promoter assay demonstrated that both JQ1 and Brd4 siRNA inhibited TGF-β1-induced Nox4 promoter activity. (Fig. 7D). Collectively, these results indicated that Brd4 inhibited Nox4 through the upstream Smad3 and
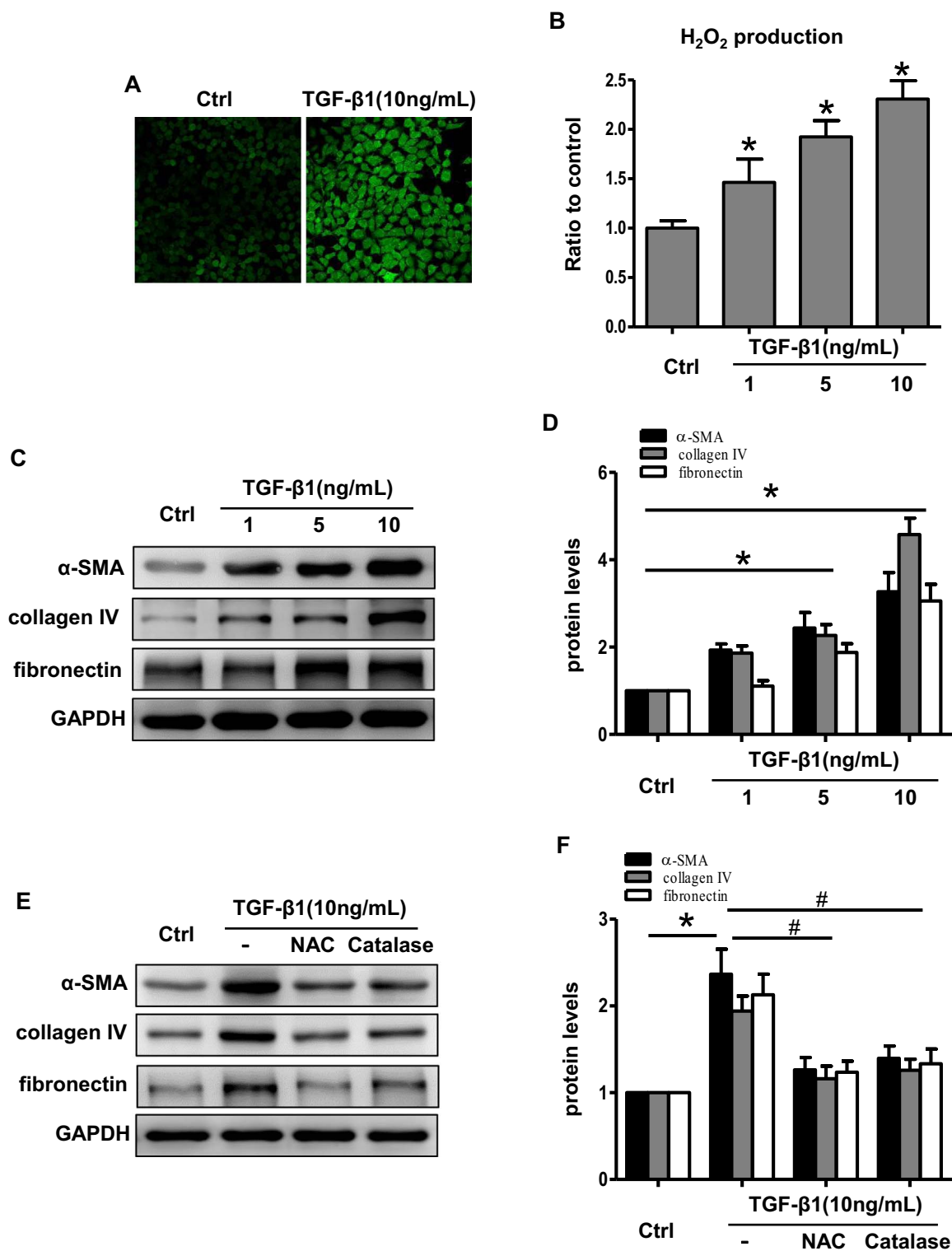
**Fig. 4.** TGF-β1-induced renal fibrosis depends on oxidative stress. (A) In HK-2 cells, TGF-β1 (10 ng/mL) increased the generation of ROS detected with DCFH-DA. Representing image fields from three independent experiments. (B) HK-2 cells were treated with TGF-β1 (0, 1, 5, 10 ng/mL) for 24 h. An Amplex Red assay shows that hydrogen peroxide was increased with the TGF-β1 concentration. Bar graphs showing the fold changes in $H_2O_2$ relative to the control group from three independent experiments, each performed in triplicate. *$P < 0.05$ relative to control group. (C) Collagen IV, α-SMA and fibronectin protein levels were detected in HK-2 cells treated with TGF-β1 (0, 1, 5, 10 ng/mL) for 24 h. (D) Protein levels were quantified by densitometry and normalized to the expression of GAPDH from three independent experiments. * $P < 0.05$ versus the control group. (E-F) HK-2 cells were pretreated with 50 U/mL PEG-catalase or 5 mM N-acetyl-cysteine (NAC) for 1 h, and then 10 ng/mL TGF-β1 was added for 24 h. The protein expression levels of collagen IV, α-SMA and fibronectin were determined by Western blotting. Protein levels were quantified by densitometry and normalized to the expression of GAPDH from three independent experiments. *$P < 0.05$ versus the control group; #$P < 0.05$ versus the TGF-β1 group.
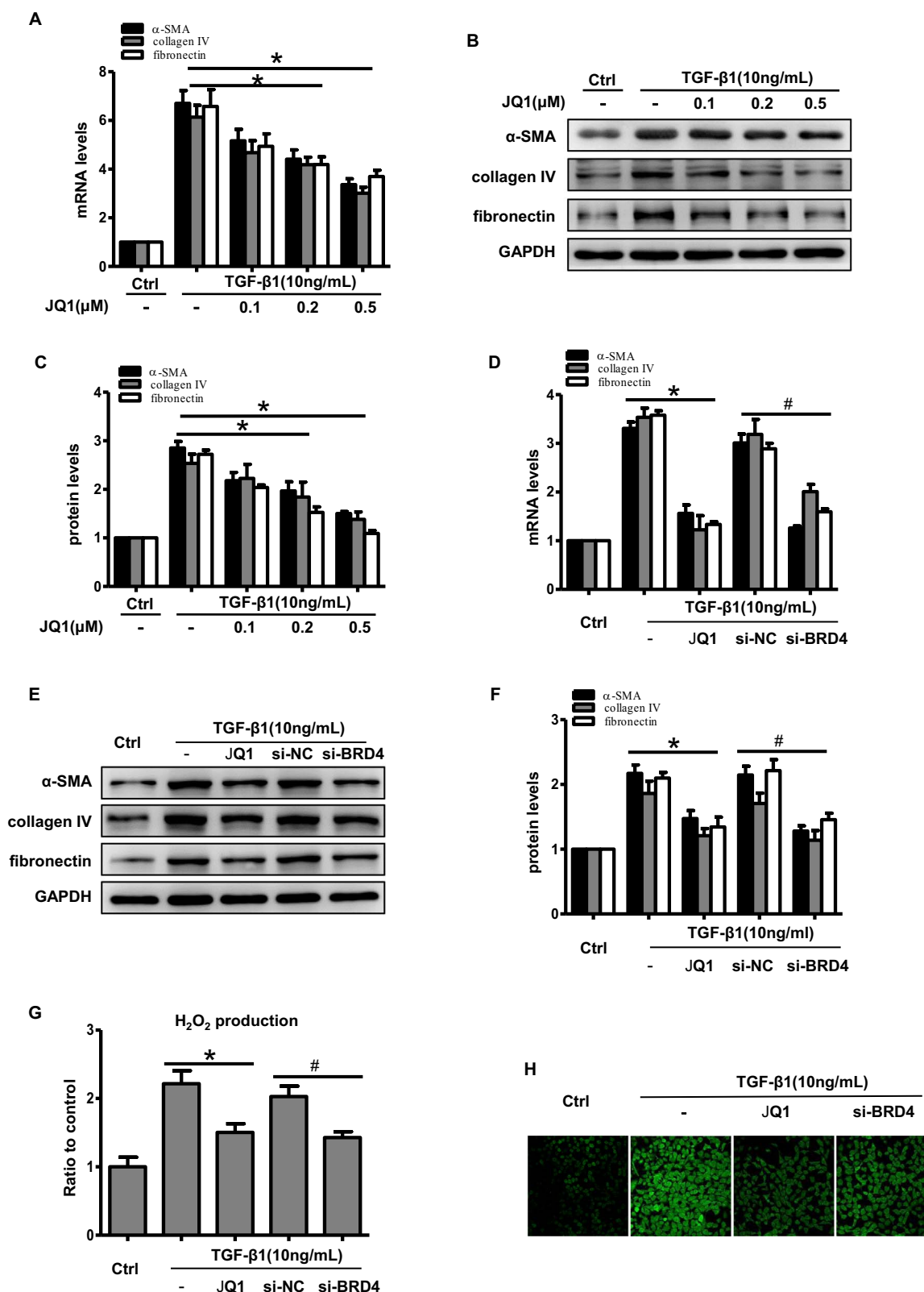
**Fig. 5.** Brd4 inhibition attenuated TGF-β1-induced fibrosis and oxidative stress in HK-2 cells. (A-C) HK-2 cells were pretreated with or without JQ1 at different doses (0.1, 0.2, 0.5 μM) for 1 h, and then treated with TGF-β1 (10 ng/mL) for 24 h. (A) Real-time PCR analyses for the mRNA expression of collagen IV, α-SMA and fibronectin. *P < 0.05 versus the TGF-β1 group. Bar graphs represent three independent experiments, each performed in triplicates. (B) Western blot analyses for the protein expression of collagen IV, α-SMA and fibronectin. (C) Protein levels were quantified by densitometry and normalized to the expression of GAPDH from three independent experiments. *P < 0.05 versus the TGF-β1 group. (D-H) HK-2 cells were transfected with an siRNA against Brd4 or a negative control siRNA (si-NC) for 48 h or pretreated with 0.5 μM JQ1 for 1 h, and then treated with TGF-β1 (10 ng/mL) for 24 h. (D) Real-time PCR analyses for the mRNA expression of collagen IV, α-SMA and fibronectin in the indicated group. Bar graphs represent three independent experiments, each performed in triplicates. *P < 0.05 versus TGF-β1; #P < 0.05 versus si-NC. (E) Western blot analyses for the protein expression of collagen IV, α-SMA, and fibronectin in the indicated group. (F) Protein levels were quantified by densitometry and normalized to the expression of GAPDH from three independent experiments. * P < 0.05 versus TGF-β1; #P < 0.05 versus si-NC. (G) H₂O₂ production in HK-2 cells in the indicated groups. Bar graphs represent three independent experiments, each performed in triplicates. * P < 0.05 versus TGF-β1; #P < 0.05 versus si-NC. (H) Representative images showing ROS stained with DCFH-DA dye in the indicated groups from three independent experiments.
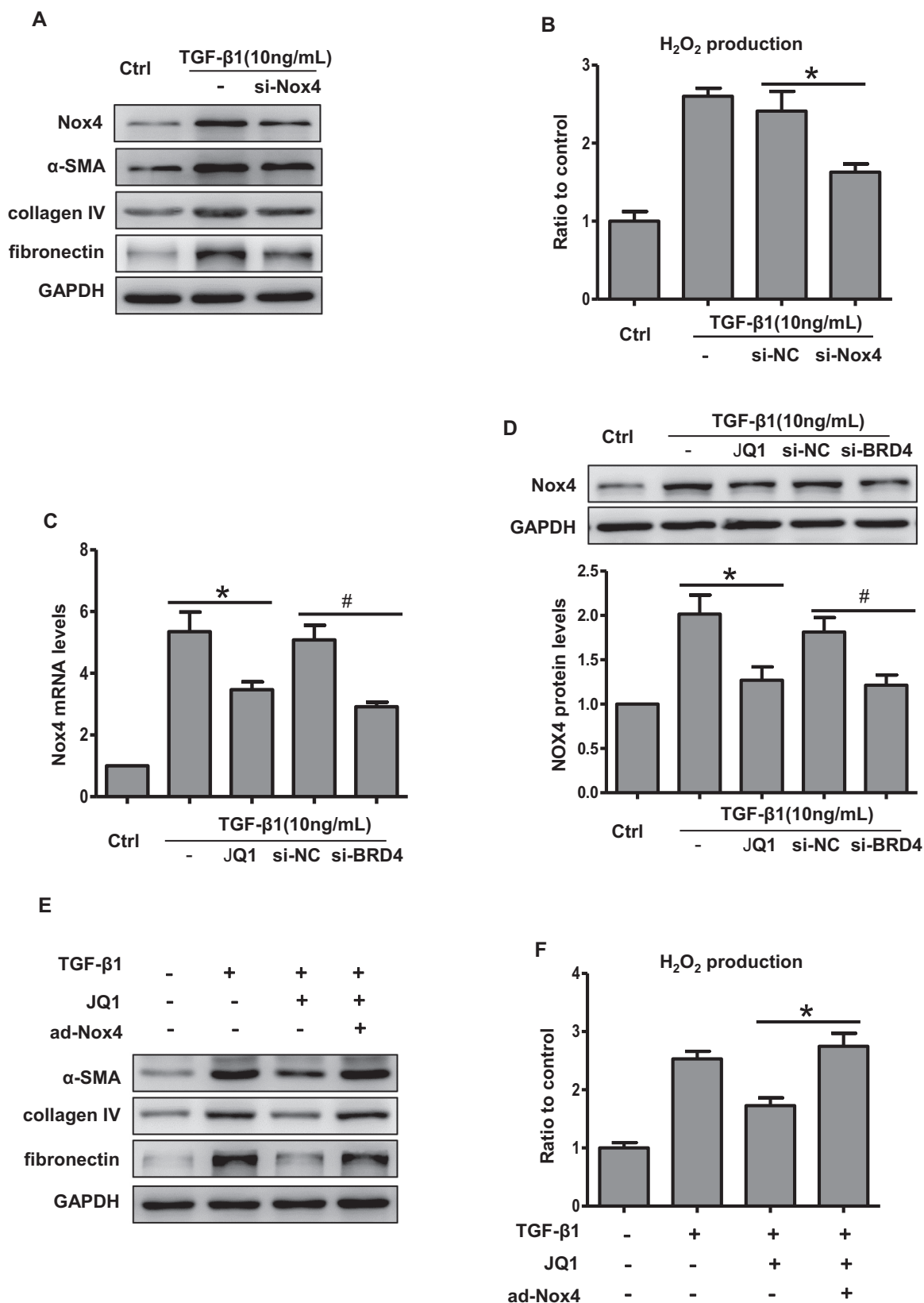
**Fig. 6.** Brd4 inhibition blocked Nox4-mediated ROS and fibrosis in HK-2 cells. (A) Representative bands of Western blot analyses for the expression of Nox4, collagen IV, α-SMA, and fibronectin in the presence of TGF-β1 or siRNA against Nox4 from three independent experiments. (B) $H_2O_2$ production measured by Amplex Red in HK-2 cells transfected with siRNA against Nox4 or a negative control siRNA in the presence or absence of TGF-β1. Bar graphs represent three independent experiments, each performed in triplicates. *$P < 0.05$ versus si-NC. (C) Real-time PCR analyses for the mRNA expression of Nox4 under the condition indicated from three independent experiments, each performed in triplicates. *$P < 0.05$ versus TGF-β1; #$P < 0.05$ versus si-NC. (D) Western Blot analyses for the protein expression of Nox4 and bar graph quantification as indicated from three independent experiments. *$P < 0.05$ versus TGF-β1; #$P < 0.05$ versus si-NC. (E-F) HK-2 cells were treated with TGF-β1 (10 ng/mL) for 24 h in the presence or absence of JQ1. TGF-β1+JQ1-treated HK-2 cells were then infected with adenovirus carrying the human Nox4 for 48 h. (E) Representative Western blot analyses of collagen IV, α-SMA and fibronectin in the indicated groups. (F) $H_2O_2$ production measured by Amplex Red in HK-2 cells in the indicated groups. Bar graphs represent three independent experiments, each performed in triplicates. *$P < 0.05$ versus the TGF-β1+JQ1 group.
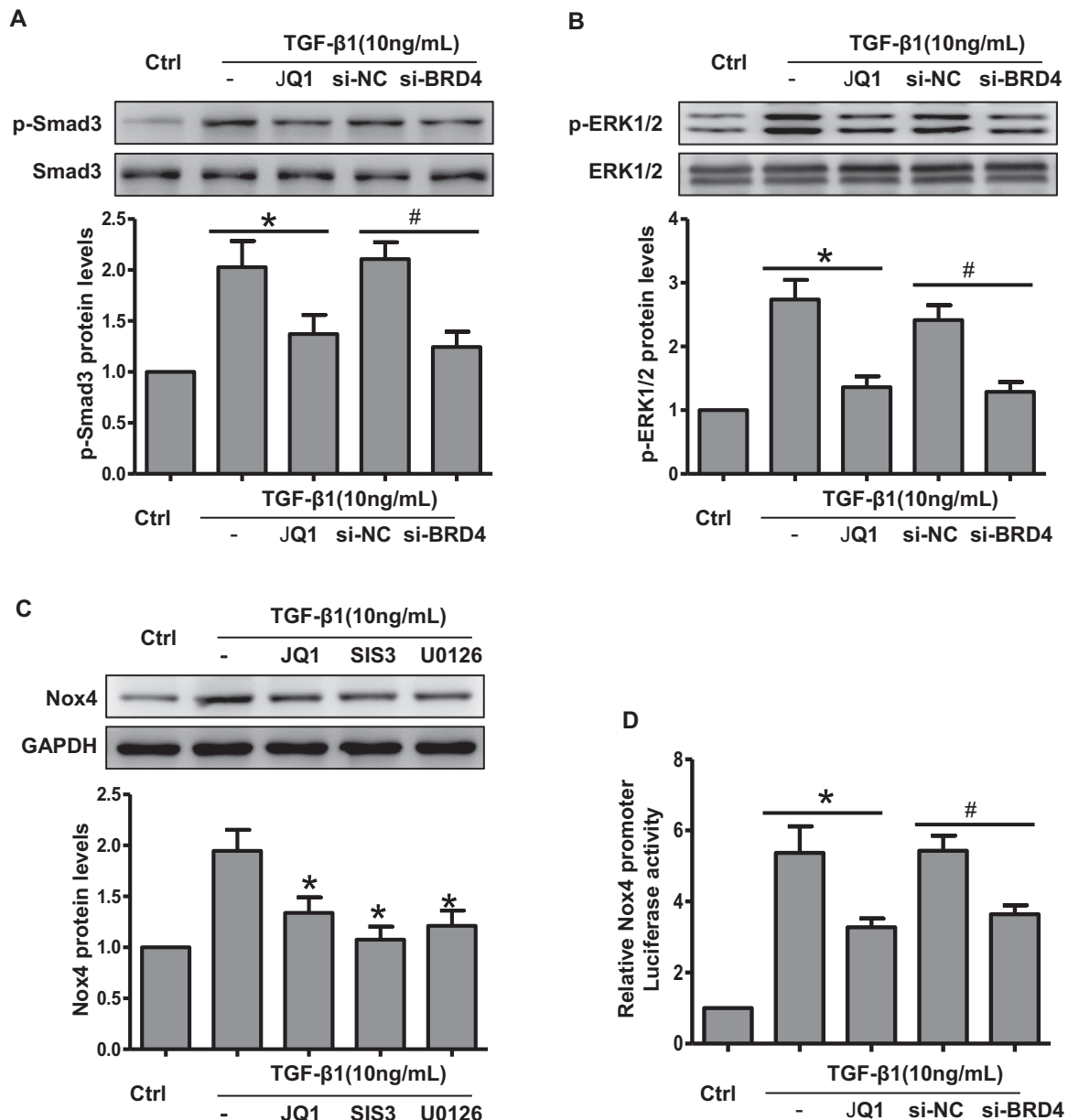
**Fig. 7.** Brd4 regulated Nox4 expression via the Smad and ERK pathways. (A) Western blot analyses for the protein expression of Smad3 and phosphorylated Smad3 in the indicated groups and quantitative analysis of Smad3 phosphorylation. *$P < 0.05$ versus TGF-β1, #$P < 0.05$ versus si-NC. (B) Western blot analyses for the protein expression of ERK1/2 and phosphorylated ERK1/2 in the indicated groups and quantitative analysis of ERK1/2 phosphorylation. *$P < 0.05$ versus TGF-β1, #$P < 0.05$ versus si-NC. (C) HK-2 cells were pretreated with either JQ1 (0.5 µM), SIS3 (Smad3 inhibitor, 10 µM) or U0126 (ERK1/2 inhibitor,10 µM) for 1 h and then treated with TGF-β1 (10 ng/mL) for 24 h. Western blot analyses for the protein expression of Nox4 in the indicated groups and quantification. *$P < 0.05$ versus TGF-β1. (A-C) Each Western blot analysis is from three independent experiments. (D) Luciferase assay of Nox4 promoter activity in the presence of JQ1 or Brd4 knockdown with siRNA from three independent experiments, each performed in six replicates. *$P < 0.05$ versus TGF-β1, #$P < 0.05$ versus si-NC.

ERK1/2 pathways and then transcriptionally decreased the Nox4 promoter activity.

### 3.7. JQ1 attenuated Nox4-mediated oxidative stress and Smad/ERK signaling in vivo

To recapitulate the in vitro findings of the effect of Brd4 regulation on Nox4-induced ROS, we tested the effects of JQ1 on UUO-induced oxidative stress. JQ1 significantly suppressed UUO-induced hydrogen peroxide production (Fig. 8A). Nox4 protein levels were also significantly increased in UUO tissues compared with the sham group (Fig. 8B). JQ1 treatment alleviated the increase in Nox4 expression in UUO rats (Fig. 8B). Additionally, the Smad/ERK signaling pathways involved in TGF-β1-induced Nox4 expression were activated by UUO

and were inhibited in the UUO rats that received JQ1 (Fig. 8C and D). Together, these results supported the hypothesis that Brd4 inhibition prevented UUO-induced fibrosis through blocking Smad/ERK signaling and Nox4-dependent ROS generation.

## 4. Discussion

In this study, we demonstrated that Brd4 inhibition attenuated TGF-β1-induced fibrotic gene expression and UUO-induced renal fibrosis. The Brd4 inhibitor JQ1 could block and even reverse the progression of renal fibrosis. Consistently, TGF-β1-induced fibrotic gene expression and Nox4-mediated ROS generation were also blocked by Brd4 knockdown or JQ1. Further, Brd4 modulated the transcriptional activity of Nox4, and this regulation occurred through the Smad3
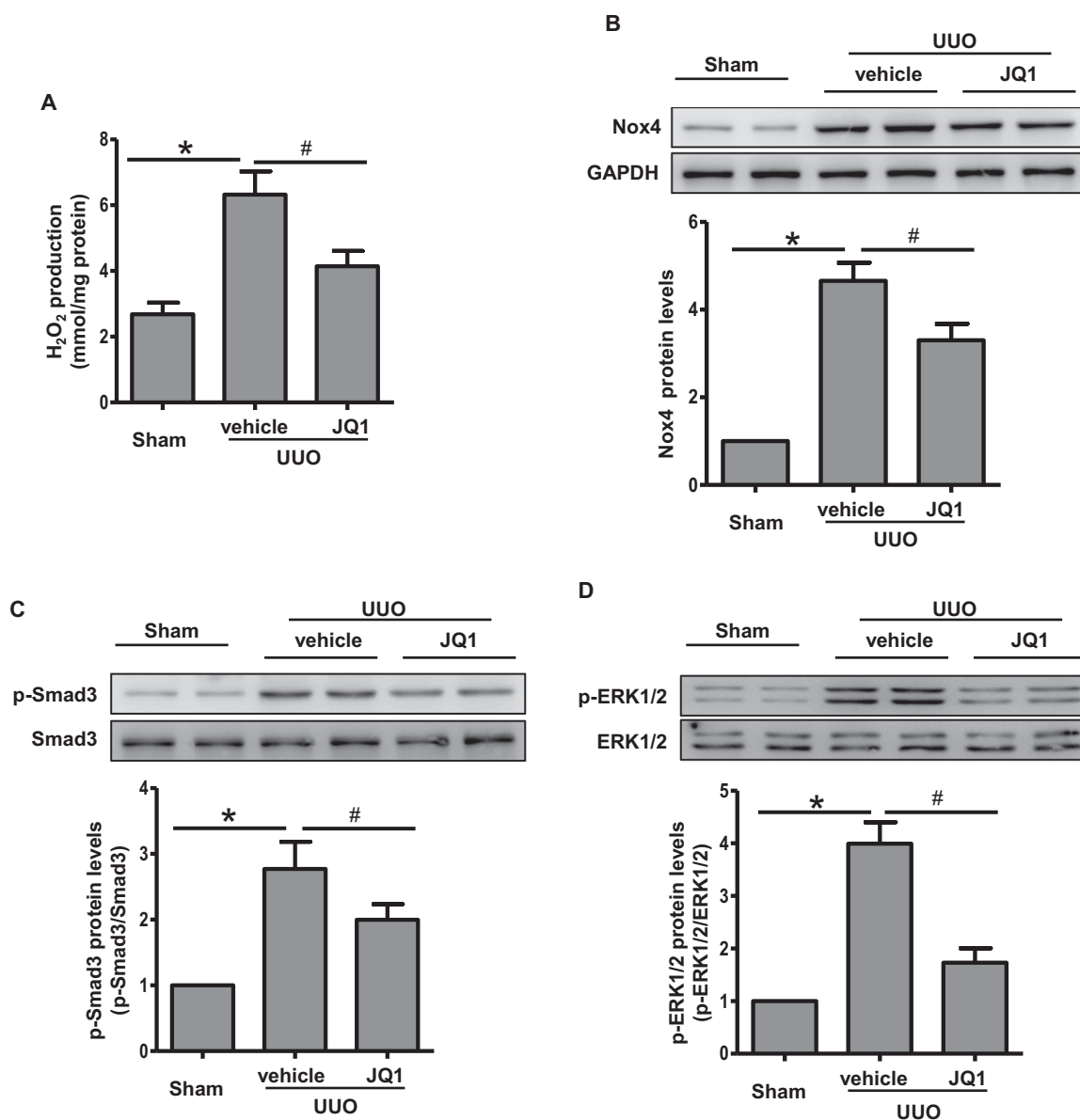
**Fig. 8.** JQ1 attenuated Nox4-mediated oxidative stress and Smad/ERK signaling in vivo. (A) $H_2O_2$ production in UUO rats treated with JQ1 or vehicle. (B) Western blot analyses for the protein expression of Nox4 in UUO rats treated with JQ1 or vehicle at day 7 and quantification. (C) Western blot analyses for the protein expression of Smad3 and phosphorylated Smad3 in UUO rats treated with JQ1 or vehicle at day 7 and quantification. (D) Western blot analyses for the protein expression of ERK1/2 and phosphorylated ERK1/2 in UUO rats treated with JQ1 or vehicle at day 7 and quantification. *$P < 0.05$ versus sham group, #$P < 0.05$ versus vehicle group, n=4 in each group.

and ERK signaling pathways. Therefore, our study indicated that Brd4 might be a potential therapeutic target for renal fibrosis and that JQ1 might be an attractive agent for renal fibrosis treatment.

Epigenetic mechanisms, including histone acetylation, have been reported to be involved in the progression from acute kidney injury to chronic kidney diseases [24]. The histone acetylation state is regulated by the activity of histone acetylases and deacetylases, which have been implicated as key regulators of diabetes- and TGF-β1-induced renal fibrosis [25,26]. Brd4, as a relatively well-studied BET member, recognizes the histone acetylation tag and facilitates chromatin targeting and transcription machinery assembly. In light of its potentially potent roles, Brd4 has been investigated in different kidney diseases.

Suarez-Alvarez B et al. explored renal damage in several different experimental animal models including unilateral ureteral obstruction and found that JQ1 reduced the transcription of proinflammatory genes by dampening nuclear RelA NF-kB levels [10]. In the UUO model, they further showed that JQ1 diminished the presence of infiltrating monocytes/macrophages and reduced the direct binding

of Brd4 to pro-inflammatory gene promoters [10]. Consistently, BET bromodomain inhibition ameliorated HIV-associated nephropathy by suppressing NF-κB-mediated inflammation [7]. However, the direct effect of JQ1 on the severity and underlying mechanisms of renal fibrosis was not mentioned. In our study, we confirmed that the Brd4 inhibitor JQ1 delayed the progression of renal fibrosis and ameliorated established renal fibrosis. Meanwhile, a great body of evidence has shown that NF-κB is tightly related to renal fibrosis. Therefore, studies demonstrating the blockade of the NF-κB pathway and reduced inflammatory cell infiltration might support our finding [7,10].

TGF-β1 is a pleiotropic cytokine produced during fibrogenesis in the kidney. TGF-β1 is up-regulated during epithelial-mesenchymal transition (EMT) and UUO-induced renal fibrosis. TGF-β1-enhanced renal fibrosis depends on downstream Smad3 signaling [27]. Although Smad2 is also strongly activated in human fibrotic kidney diseases, it is now well recognized that Smad3 is the imperative mediator of TGF-β1-induced EMT and tissue fibrosis [28–30]. In our study, we observed Smad3 phosphorylation in TGF-β1-treated HK-2 cells. Considering the

central role of TGF-β/Smad signaling during renal fibrosis, many inhibitors have been developed and have shown impressive renal protection after obstructive injury [2,30]. Here, we linked the epigenetic molecule Brd4 with TGF-β/Smad signaling. Our data demonstrated that Brd4 was induced in UUO renal tissue, in which TGF-β1 acts as the master regulator during fibrosis. Further, the use of the Brd4 chemical inhibitor JQ1 alleviated the severity of the nephropathy and inhibited Smad3 activation. The deactivation of TGF-β/Smad3 signaling might explain the anti-fibrotic effects of JQ1. Consequently, we observed that fibrotic genes such as α-SMA, collagen IV and fibronectin were down-regulated by JQ1 or Brd4 knockdown. Consistent with previous reports [30], the Smad3 phosphorylation inhibitor SIS3 suppressed TGF-β1-induced fibrotic gene expression. However, whether Brd4 regulates TGF-β1 expression was not raveled in this study. Based on the alleviation of renal fibrosis by JQ1 and the association between renal fibrosis and TGF-β1 levels, we speculated that Brd4 might decrease the renal TGF-β1 expression. It is worth great efforts to investigate whether Brd4 recruits to TGF-β1 promoter or enhancer region to initiate TGF-β1 transcription. Taken together, we established the regulation of TGF-β signaling by Brd4, though the underlying transcriptional mechanisms remain to be investigated.

Oxidative stress has been well established to play a crucial role in renal fibrosis. ROS are reportedly involved in activation of fibroblasts, mesangial cell hypertrophy and tubular epithelial cell migration [31,32]. In addition, ROS induce the secretion of chemokines and growth factors [32]. Different types of kidney damage, including obstructive nephropathy, result in ROS production and an elevation in TGF-β1 levels. The link between oxidative stress and TGF-β1 during renal fibrogenesis has been demonstrated [33]. TGF-β1 triggers ROS generation in the kidney, whereas the generated ROS in turn enhance TGF-β1-related fibrotic gene expression. Herein, we replicated the observation of increased ROS generation along with the fibrotic response in the presence of TGF-β1 in HK-2 cells and in UUO renal tissues. We further demonstrated that JQ1 dampened TGF-β1-induced ROS levels. Therefore, the renal protective effects of JQ1 might occur through the inhibition of ROS generation induced by TGF-β signaling.

The major source of ROS in renal fibrosis is NADPH oxidases. A number of studies have indicated that NOX1 [34], NOX2 [35], and NOX4 are expressed in the kidney [21,36]. Among them, Nox4 was the most tightly associated with renal fibrosis, especially in the setting of TGF-β1 stimulation. Universally, TGF-β1 can drive Nox4 expression in many cells including renal fibroblasts, epithelial cells, vascular endothelial cells, smooth muscle cells and cardiomyocytes [37,38]. In the present study, high levels of Nox4 and its specific $H_2O_2$ product were detected in TGF-β1-treated HK-2 cells and UUO renal tissues. Brd4 inhibition suppressed Nox4 protein levels and decreased its transcriptional activity and correspondingly resulted in a reduction in $H_2O_2$ production. Furthermore, we overexpressed Nox4 in HK-2 cells, and the inhibitory effects of JQ1 on TGF-β1-induced fibrotic gene expression were blunted. Therefore, we speculated that Brd4 inhibition attenuates kidney fibrosis via the TGF-β-Nox4 pathway.

Of note, Shah AM's group employed Nox4 inducible-knockout background mice and found no disease-promoting role of Nox4 but rather a small protective effect against renal inflammation and fibrosis [15]. Nox4 is also considered to be a Janus-faced ROS generating oxidase for its dual role in physiological and pathological conditions [39,40]. The conflicting reports on Nox4 roles might be due to the levels of $H_2O_2$ produced. In physiological conditions, ROS at low levels may act as signaling molecules. The redox imbalance that occurs due to excess ROS might be deleterious.

JQ1, a potent Brd4 inhibitor, was widely used in our study. However, JQ1 has serious preclinical toxicity in vivo. It should be noted that in our in vivo Brd4 inhibition study, JQ1 might have systemic effects. More studies, especially in the tubular cell Brd4 transgenic and knockout mouse models, are warranted. Recently, a number of BET inhibitors have been developed and given in clinical

trials to patients with certain diseases, including solid tumors and hematologic malignancies [41–43]. Therefore, this experimental evidence and clinical treatment indicates that Brd4 might be a potential therapeutic target in a wide range of diseases including renal diseases.

Although the regulation of Nox4 by Brd4 was indicated, one limitation γof this study is the insufficient revelation of the working epigenetic mechanism. Reportedly, the Nox4 promoter harbors many transcription factor or coactivator binding sites, including for Smad3 [44] and NF-κB [45]. It is reasonable to hypothesize that Brd4 might block Smad3 or NF-κB binding to cis-elements in the Nox4 promoter. Regarding the histone acetylation reader property of Brd4, we could further speculate that Brd4 might facilitate these nuclear transcription factors to form transcription machinery at the Nox4 promoter. JQ1 might dissociate Brd4 from the chromatin complex and thus decrease the Nox4 transcriptional activity. Undoubtedly, the direct interaction between Brd4, transcription factors and DNA segments warrants further investigation.

In conclusion, we have identified the protective effect of a Brd4 inhibitor during UUO-induced renal fibrosis. Further, we showed that Brd4 inhibition blocked renal fibrotic gene expression by preventing TGF-β1 signaling and Nox4-dependent ROS generation. Overall, these results revealed that Brd4 is a potential therapeutic target in the treatment of renal fibrosis.

## Disclosures

None.

## Acknowledgments

## Appendix A. Supporting material

Supplementary data associated with this article can be found in the online version at http://dx.doi.org/10.1016/j.redox.2016.12.031.

## References

[1] I. Loeffler, G. Wolf, Transforming growth factor-beta and the progression of renal disease, *Nephrol. Dial. Transplant.* 29 (Suppl 1) (2014) i37–i45.
[2] X.M. Meng, D.J. Nikolic-Paterson, H.Y. Lan, TGF-beta: the master regulator of fibrosis, Nat. Rev. Nephrol. 12 (6) (2016) 325–338.
[3] X.R. Huang, A.C. Chung, X.J. Wang, K.N. Lai, H.Y. Lan, Mice overexpressing latent TGF-beta1 are protected against renal fibrosis in obstructive kidney disease, Am. J. Physiol. Ren. Physiol. 295 (1) (2008) F118–F127.
[4] J. Shi, C.R. Vakoc, The mechanisms behind the therapeutic activity of BET bromodomain inhibition, Mol. Cell 54 (5) (2014) 728–736.
[5] A. Dey, F. Chitsaz, A. Abbasi, T. Misteli, K. Ozato, The double bromodomain protein Brd4 binds to acetylated chromatin during interphase and mitosis, Proc. Natl. Acad. Sci. USA 100 (15) (2003) 8758–8763.
[6] M.K. Jang, K. Mochizuki, M. Zhou, H.S. Jeong, J.N. Brady, K. Ozato, The bromodomain protein Brd4 is a positive regulatory component of P-TEFb and stimulates RNA polymerase II-dependent transcription, Mol. Cell 19 (4) (2005) 523–534.
[7] G. Zhang, R. Liu, Y. Zhong, A.N. Plotnikov, W. Zhang, L. Zeng, E. Rusinova, G. Gerona-Nevarro, N. Moshkina, J. Joshua, P.Y. Chuang, M. Ohlmeyer, J.C. He, M.M. Zhou, Down-regulation of NF-kappaB transcriptional activity in HIV-associated kidney disease by BRD4 inhibition, J. Biol. Chem. 287 (34) (2012) 28840–28851.
[8] J.W. Kim, S.M. Jang, C.H. Kim, J.H. An, E.J. Kang, K.H. Choi, New molecular bridge between RelA/p65 and NF-kappaB target genes via histone acetyltransferase TIP60 cofactor, J. Biol. Chem. 287 (10) (2012) 7780–7791.
[9] B. Huang, X.D. Yang, M.M. Zhou, K. Ozato, L.F. Chen, Brd4 coactivates transcriptional activation of NF-kappaB via specific binding to acetylated RelA, Mol. Cell. Biol. 29 (5) (2009) 1375–1387.
[10] B. Suarez-Alvarez, J.L. Morgado-Pascual, S. Rayego-Mateos, R.M. Rodriguez, R. Rodrigues-Diez, P. Cannata-Ortiz, A.B. Sanz, J. Egido, P.L. Tharaux, A. Ortiz, C. Lopez-Larrea, M. Ruiz-Ortega, Inhibition of bromodomain and extraterminal domain family proteins ameliorates experimental renal damage, J. Am. Soc. Nephrol.: JASN (2016).
[11] J. Shi, W.A. Whyte, C.J. Zepeda-Mendoza, J.P. Milazzo, C. Shen, J.S. Roe,

J.L. Minder, F. Mercan, E. Wang, M.A. Eckersley-Maslin, A.E. Campbell, S. Kawaoka, S. Shareef, Z. Zhu, J. Kendall, M. Muhar, C. Haslinger, M. Yu, R.G. Roeder, M.H. Wigler, G.A. Blobel, J. Zuber, D.L. Spector, R.A. Young, C.R. Vakoc, Role of SWI/SNF in acute leukemia maintenance and enhancer-mediated Myc regulation, Genes Dev. 27 (24) (2013) 2648–2662.

[12] P. Filippakopoulos, J. Qi, S. Picaud, Y. Shen, W.B. Smith, O. Fedorov, E.M. Morse, T. Keates, T.T. Hickman, I. Felletar, M. Philpott, S. Munro, M.R. McKeown, Y. Wang, A.L. Christie, N. West, M.J. Cameron, B. Schwartz, T.D. Heightman, N. La Thangue, C.A. French, O. Wiest, A.L. Kung, S. Knapp, J.E. Bradner, Selective inhibition of BET bromodomains, Nature 468 (7327) (2010) 1067–1073.

[13] X. Tang, R. Peng, J.E. Phillips, J. Deguzman, Y. Ren, S. Apparsundaram, Q. Luo, C.M. Bauer, M.E. Fuentes, J.A. DeMartino, G. Tyagi, R. Garrido, C.M. Hogaboam, C.P. Denton, A.M. Holmes, C. Kitson, C.S. Stevenson, D.C. Budd, Assessment of Brd4 inhibition in idiopathic pulmonary fibrosis lung fibroblasts and in vivo models of lung fibrosis, Am. J. Pathol. 183 (2) (2013) 470–479.

[14] P. Anand, J.D. Brown, C.Y. Lin, J. Qi, R. Zhang, P.C. Artero, M.A. Alaiti, J. Bullard, K. Alazem, K.B. Margulies, T.P. Cappola, M. Lemieux, J. Plutzky, J.E. Bradner, S.M. Haldar, BET bromodomains mediate transcriptional pause release in heart failure, Cell 154 (3) (2013) 569–582.

[15] A. Babelova, D. Avaniadi, O. Jung, C. Fork, J. Beckmann, J. Kosowski, N. Weissmann, N. Anilkumar, A.M. Shah, L. Schaefer, K. Schroder, R.P. Brandes, Role of Nox4 in murine models of kidney disease, Free Radic. Biol. Med. 53 (4) (2012) 842–853.

[16] L. Hecker, R. Vittal, T. Jones, R. Jagirdar, T.R. Luckhardt, J.C. Horowitz, S. Pennathur, F.J. Martinez, V.J. Thannickal, NADPH oxidase-4 mediates myofibroblast activation and fibrogenic responses to lung injury, Nat. Med. 15 (9) (2009) 1077–1081.

[17] J.L. Barnes, Y. Gorin, Myofibroblast differentiation during fibrosis: role of NAD(P) H oxidases, Kidney Int. 79 (9) (2011) 944–956.

[18] F. Jiang, G.S. Liu, G.J. Dusting, E.C. Chan, NADPH oxidase-dependent redox signaling in TGF-beta-mediated fibrotic responses, Redox Biol. 2 (2014) 267–272.

[19] X. Guan, L. Nie, T. He, K. Yang, T. Xiao, S. Wang, Y. Huang, J. Zhang, J. Wang, K. Sharma, Y. Liu, J. Zhao, Klotho suppresses renal tubulo-interstitial fibrosis by controlling basic fibroblast growth factor-2 signalling, J. Pathol. 234 (4) (2014) 560–572.

[20] X. Tong, A.R. Khandelwal, Z. Qin, X. Wu, L. Chen, T. Ago, J. Sadoshima, R.A. Cohen, Role of smooth muscle Nox4-based NADPH oxidase in neointimal hyperplasia, J. Mol. Cell. Cardiol. 89 (Pt B) (2015) 185–194.

[21] K.J. Jung, K.J. Min, J.W. Park, K.M. Park, T.K. Kwon, Carnosic acid attenuates unilateral ureteral obstruction-induced kidney fibrosis via inhibition of Akt-mediated Nox4 expression, Free Radic. Biol. Med. 97 (2016) 50–57.

[22] L. Yang, M. Qu, Y. Wang, H. Duan, P. Chen, Y. Wang, W. Shi, P. Danielson, Q. Zhou, Trichostatin A inhibits transforming growth factor-beta-induced reactive oxygen species accumulation and myofibroblast differentiation via enhanced NF-E2-related factor 2-antioxidant response element signaling, Mol. Pharmacol. 83 (3) (2013) 671–680.

[23] N. Manickam, M. Patel, K.K. Griendling, Y. Gorin, J.L. Barnes, RhoA/Rho kinase mediates TGF-beta1-induced kidney myofibroblast activation through Poldip2/ Nox4-derived reactive oxygen species, Am. J. Physiol. Ren. Physiol. 307 (2) (2014) F159–F171.

[24] R. Rodriguez-Romo, N. Berman, A. Gomez, N.A. Bobadilla, Epigenetic regulation in the acute kidney injury (AKI) to chronic kidney disease transition (CKD), Nephrology (2015).

[25] H. Noh, E.Y. Oh, J.Y. Seo, M.R. Yu, Y.O. Kim, H. Ha, H.B. Lee, Histone deacetylase-2 is a key regulator of diabetes- and transforming growth factor-beta1-induced renal injury, Am. J. Physiol. Ren. Physiol. 297 (3) (2009) F729–F739.

[26] N. Liu, S. He, L. Ma, M. Ponnusamy, J. Tang, E. Tolbert, G. Bayliss, T.C. Zhao, H. Yan, S. Zhuang, Blocking the class I histone deacetylase ameliorates renal fibrosis and inhibits renal fibroblast activation via modulating TGF-beta and EGFR signaling, PLoS One 8 (1) (2013) e54001.

[27] M. Sato, Y. Muragaki, S. Saika, A.B. Roberts, A. Ooshima, Targeted disruption of TGF-beta1/Smad3 signaling protects against renal tubulointerstitial fibrosis induced by unilateral ureteral obstruction, J. Clin. Investig. 112 (10) (2003) 1486–1494.

[28] F. Verrecchia, L. Vindevoghel, R.J. Lechleider, J. Uitto, A.B. Roberts, A. Mauviel, Smad3/AP-1 interactions control transcriptional responses to TGF-beta in a promoter-specific manner, Oncogene 20 (26) (2001) 3332–3340.

[29] L. Vindevoghel, R.J. Lechleider, A. Kon, M.P. de Caestecker, J. Uitto, A.B. Roberts, A. Mauviel, SMAD3/4-dependent transcriptional activation of the human type VII collagen gene (COL7A1) promoter by transforming growth factor beta, Proc. Natl. Acad. Sci. USA 95 (25) (1998) 14769–14774.

[30] J. Ai, J. Nie, J. He, Q. Guo, M. Li, Y. Lei, Y. Liu, Z. Zhou, F. Zhu, M. Liang, Y. Cheng, F.F. Hou, GQ5 hinders renal fibrosis in obstructive nephropathy by selectively inhibiting TGF-beta-induced Smad3 phosphorylation, J. Am. Soc. Nephrol.: JASN 26 (8) (2015) 1827–1838.

[31] Y. Liu, Cellular and molecular mechanisms of renal fibrosis, Nat. Rev. Nephrol. 7 (12) (2011) 684–696.

[32] K. Richter, A. Konzack, T. Pihlajaniemi, R. Heljasvaara, T. Kietzmann, Redox-fibrosis: Impact of TGFbeta1 on ROS generators, mediators and functional consequences, Redox Biol. 6 (2015) 344–352.

[33] T. Qin, S. Yin, J. Yang, Q. Zhang, Y. Liu, F. Huang, W. Cao, Sinomenine attenuates renal fibrosis through Nrf2-mediated inhibition of oxidative stress and TGFbeta signaling, Toxicol. Appl. Pharmacol. 304 (2016) 1–8.

[34] K. Zhu, T. Kakehi, M. Matsumoto, K. Iwata, M. Ibi, Y. Ohshima, J. Zhang, J. Liu, X. Wen, A. Taye, C. Fan, M. Katsuyama, K. Sharma, C. Yabe-Nishimura, NADPH oxidase NOX1 is involved in activation of protein kinase C and premature senescence in early stage diabetic kidney, Free Radic. Biol. Med. 83 (2015) 21–30.

[35] J. Qin, W.J. Mei, Y.Y. Xie, L. Huang, Q.J. Yuan, G.Y. Hu, L.J. Tao, Z.Z. Peng, Fluorofenidone attenuates oxidative stress and renal fibrosis in obstructive nephropathy via blocking NOX2 (gp91phox) expression and inhibiting ERK/MAPK signaling pathway, Kidney blood Press. Res. 40 (1) (2015) 89–99.

[36] M. Sedeek, R. Nasrallah, R.M. Touyz, R.L. Hebert, NADPH oxidases, reactive oxygen species, and the kidney: friend and foe, J. Am. Soc. Nephrol.: JASN 24 (10) (2013) 1512–1518.

[37] V. Thallas-Bonke, K.A. Jandeleit-Dahm, M.E. Cooper, Nox-4 and progressive kidney disease, Curr. Opin. Nephrol. Hypertens. 24 (1) (2015) 74–80.

[38] A. Konior, A. Schramm, M. Czesnikiewicz-Guzik, T.J. Guzik, NADPH oxidases in vascular pathology, Antioxid. Redox Signal. 20 (17) (2014) 2794–2814.

[39] K. Schroder, M. Zhang, S. Benkhoff, A. Mieth, R. Pliquett, J. Kosowski, C. Kruse, P. Luedike, U.R. Michaelis, N. Weissmann, S. Dimmeler, A.M. Shah, R.P. Brandes, Nox4 is a protective reactive oxygen species generating vascular NADPH oxidase, Circ. Res. 110 (9) (2012) 1217–1225.

[40] H.H. Schmidt, K. Wingler, C. Kleinschnitz, G. Dusting, NOX4 is a Janus-faced reactive oxygen species generating NADPH oxidase, Circ. Res. 111 (1) (2012) e15–e16 (author reply e 17-e18).

[41] V. Sahai, A.J. Redig, K.A. Collier, F.D. Eckerdt, H.G. Munshi, Targeting bet bromodomain proteins in solid tumors, Oncotarget 7 (33) (2016) 53997–54009.

[42] A. Chaidos, V. Caputo, A. Karadimitris, Inhibition of bromodomain and extra-terminal proteins (BET) as a potential therapeutic approach in haematological malignancies: emerging preclinical and clinical evidence, Ther. Adv. Hematol. 6 (3) (2015) 128–141.

[43] S.G. Smith, M.M. Zhou, The Bromodomain: a new target in emerging epigenetic, Med. ACS Chem. Biol. 11 (3) (2016) 598–608.

[44] G. Bai, T.D. Hock, N. Logsdon, Y. Zhou, V.J. Thannickal, A far-upstream AP-1/ Smad binding box regulates human NOX4 promoter activation by transforming growth factor-beta, Gene 540 (1) (2014) 62–67.

[45] X. Lu, T.C. Murphy, M.S. Nanes, C.M. Hart, PPARγ regulates hypoxia-induced Nox4 expression in human pulmonary artery smooth muscle cells through NF-κB, Am. J. Physiol. Lung Cell. Mol. Physiol. 299 (4) (2010) L559–L566.